

Garold L. Gresham,¹ B.Sc.; Gary S. Groenewold,¹ Ph.D.; William F. Bauer,¹ Ph.D. and
Jani C. Ingram,¹ Ph.D.

Secondary Ion Mass Spectrometric Characterization of Nail Polishes and Paint Surfaces*

REFERENCE: Gresham GL, Groenewold GS, Bauer WF, Ingram JC. Secondary ion mass spectrometric characterization of nail polishes and paint surfaces. *J Forensic Sci* 2000;45(2):310–323.

ABSTRACT: A variety of paint and fingernail polish samples, which were visually similar, but had different chemical compositions and formulations, was analyzed using quadrupole static secondary ion mass spectrometry (SIMS). Coating distinction was easily achieved in many cases because of the presence of dominant ions derived from the components of the coating, which could be observed in the SIMS spectra. In other instances, coating distinction was difficult within a product line because of spectral complexity; for this reason and because of the large numbers of spectra generated in this study, multivariate statistical techniques were employed, which allowed the meaningful classification and comparison of spectra. Partial Least Squares (PLS) and Principal Component Analysis (PCA) were applied to quadrupole SIMS data. PCA showed distinct spectral differences between most spectral groups, and also emphasized the reproducibility of the SIMS spectra. When using PLS analysis, reasonably accurate coating identification was achieved with the data. Overall, the PLS model is more than 90% effective in identifying the spectrum of a particular coating, and nearly 100% effective at telling which coating components represented in the PLS models are not present in a spectrum. The level of spectral variation caused by sample bombardment in the SIMS analysis was investigated using Fourier transform infrared spectroscopy (FT-IR) and quadrupole static SIMS. Changes in the FT-IR spectra were observed and were most likely a result of a number of factors involving the static SIMS analysis. However, the bulk of the sample is unaltered and may be used for further testing.

KEYWORDS: forensic science, paint, nail polish, static secondary ion mass spectrometry

The rapid characterization and differentiation of small, discrete samples that comprise trace physical evidence remains problematic despite their importance in linking an individual to a specific location or criminal act. Trace physical evidence consists of minute quantities of materials such as hair, fibers, soil particles, glass, paint chips, or plant material, which are sometimes as small as only a few μm^2 or mm^2 . Chemical analysis of trace samples is challenging because of the limited size of the sample, the limited number of discrete samples available, and the small absolute quantities of analyte compounds present in the samples. These difficulties

have resulted in the application of a large number of characterization approaches, each of which offers distinct advantages over others, but also have definite limitations, including lack of specificity and the consumption or destruction of the sample during testing. Classical visual microscopy is an often used technique, because a high level of expertise has been developed, and because it is non-destructive. Microscopy reveals the physical aspects of trace evidence, which includes characteristics such as color, size, shape, inclusions, surface debris, damage, refractive index, and variations in the characteristics within a sample (1–3). The limitation of the technique is that small samples at times cannot be distinguished from one another even though their chemical compositions may be very dissimilar. Also surface contamination at minute levels is undetectable with visual microscopy. The obvious way to surmount these problems is to resort to chemical characterization.

Investigations of the optical properties of a trace sample generate chemical information in a manner that is typically nondestructive. There is a variety of spectroscopic approaches, which include microspectrophotometry (4,5), infrared (IR) spectroscopy (6–9), IR microscopy (10,11), Raman spectroscopy (10,12), and fluorescence (13). When IR or fluorescence spectra can be generated, the chemical characterization can be very unique; however, the drawback to spectroscopic investigation is that the sample must have absorption or fluorescence peaks in unique regions of the optical spectrum, which frequently is not the case. Also these techniques can be insufficiently sensitive for small samples unless specialized sample holders or attachments are used.

A more sensitive chemical characterization of trace samples can be generated using more destructive analytical techniques. These include extraction-gas chromatography (1), pyrolysis-gas chromatography (8,14–16), pyrolysis-mass spectrometry (8), pyrolysis-gas chromatography/mass spectrometry (14), thin layer chromatography (17), high performance liquid chromatography (18), and other hybridized instrumental techniques (16,19). Elemental characterization of trace samples has been achieved using scanning electron microscopy (SEM) with energy dispersive X-ray analysis (EDXA) (20,21). The coating industry, specifically, has applied a number of analytical techniques to ensure that the needed characteristics are present on a coating surface. These techniques include X-ray photoelectron spectroscopy and atomic force microscopy as well as SEM with EDXA (22).

Classical techniques such as density measurements, melting points, solvent solubility and chemical tests are also used to characterize trace evidence (1,23,24). These approaches are capable of excellent chemical selectivity provided sufficient sample is avail-

¹ Idaho National Engineering and Environmental Laboratory, Idaho Falls, ID 83415-2208.

* The National Institute of Justice has provided funding for this research. Received 29 Jan. 1999; and in revised form 1 June 1999; accepted 2 June 1999.

able. However, the drawbacks of these techniques are that their sensitivity is inadequate for microgram-sized samples, and that the samples are consumed or destroyed as a result of the analysis, preventing any additional testing.

Static secondary ion mass spectrometry (SIMS) is a sensitive and nearly nondestructive approach to the characterization of small samples of paint and other coating materials, that is capable of generating specific chemical information (molecular and atomic). Static SIMS has been applied to the analysis of small samples of automotive paints and fingernail polishes. The operating principle behind static SIMS is simple: the trace sample is bombarded with a high-energy projectile, which can be monoatomic or polyatomic. Intact molecules, their fragments, and atoms are "sputtered" from the surface; some fraction of these are ionized, and hence can then be mass measured and detected using a variety of mass analyzers. The term "static" implies that the degree of surface bombardment (referred to as dose, ions/cm²) is low enough that the chemical composition of the surface is unaltered (25). In our laboratory this technique has been applied to the detection of organophosphates (26–28), organosulfides (29,30), organic amines (31,32), and metal cyanides (33) on substrates including soil, rock, vegetation, and metal surfaces.

Historically, static SIMS has had broad applicability for the characterization of polymers, and extensive libraries of polymer SIMS spectra have been compiled (34,35). However, static SIMS polymer libraries have not addressed the specific need for differentiation and characterization of samples of forensic interest, nor has the utility of static SIMS been evaluated for this specific application. Because SIMS instruments are capable of analyzing very small samples, application to trace sample analysis is an obvious extension. The present report describes the application of static SIMS to the characterization and differentiation of coating samples, specifically automotive paints, spray paints and fingernail polishes. The results show that in most cases the coatings can be differentiated by manufacturer, and frequently to the specific coating product.

Experimental

Instrumentation

The SIMS instrument used in this study was based on an Extrel (Pittsburgh, PA) triple quadrupole mass spectrometer, with a mass range of 10 to 600 amu. The instrument was configured with a ReO₄⁻ primary ion gun mounted on a 12-in. (30.48 cm) spherical vacuum chamber at a 35-deg angle relative to the axis of the secondary ion mass spectrometer. The placement of the primary gun allows the primary beam to pass through the center of the spherical chamber. The ion gun was operated at 5.25 keV with a primary ion current between 200 and 300 pA. Typical primary ion doses were on the order of 3.6×10^{12} ions/cm² (36). Typical pressure in the spherical chamber was 3×10^{-7} Torr. The primary ion current could be measured using a retractable Faraday cup, which could be inserted into a position colinear with the axis of the secondary ion mass spectrometer.

The secondary anions and cations were alternately extracted from the sample target region at 0.2 amu intervals using pulsed secondary ion extraction (37), which operates by alternating the polarity of the secondary ion extraction lens from positive to negative. This mitigates the sample charge buildup on the sample surface and also allows for the simultaneous collection of both positive and negative ion spectra from a single analytical run. Good sensitivity was obtained for all coating materials with total ion currents for

some coating samples greater than 425 000 counts per second (maximum instrument count limit is 450 000 counts per second).

Reflectance infrared spectra were recorded using a Digilab FTS-65 Fourier transform infrared spectrometer (BioRad Corp., Cambridge, MA) equipped with a Spectra-Tech IR-PlanTM infrared (IR) microscope (Stanford, CT) and a Spectra-Tech 15X Refflachromat IR objective. The spectra consisted of 256 co-added scans at a resolution of 4 cm⁻¹. A narrow-band liquid nitrogen (LN₂) cooled mercury cadmium telluride (MCT) detector was employed and spectra were collected between 4400 to 800 cm⁻¹. The IR sample spot size was set at 300 × 300 μm (square spot size). The unpainted side of the SIMS sample target was used as the reference.

Samples

Automotive paints, automotive touch-up paints, aerosol spray paints and fingernail polish samples (Table 1) used in the present study were obtained from local retail suppliers. DuPont base coat paints used in the study were formulated on-site by the automotive paint supplier. All spray paint samples were received as a ~4 × 4 in. (10 × 10 cm) coated area on aluminum foil. The painted area of aluminum foil was folded back on itself to prevent contamination of the paint surface. The fingernail polish and automotive paint samples were obtained as liquids. Single-layer coating samples (≥150 μm sample thickness) were applied directly on to the SIMS steel sample targets for analysis and allowed to air dry for the quadrupole SIMS, and FT-IR analysis. Drying times varied for the different coatings (i.e., finger nail polish samples required short drying time compared to the Dupont automotive paints). A number of samples were prepared for each coating and allowed to weather. Samples were analyzed over an 8 to 12 month period after sample preparation. No further sample preparation was required for the liquid samples.

The paint samples were cut from the aluminum foil, and attached to the sample holder using double-sided tape. The nominal sample size for the broad beam quadrupole SIMS was 2 × 3 mm; the instrument is capable of analyzing samples as small as 100 μm in width to slightly less than 0.5 in. (1.27 cm) in width.

Results and Discussion

Quadrupole SIMS Spectral of Coatings from Various Manufacturer Products

Figure 1 shows a series of quadrupole SIMS spectra in which the positive ions are plotted above the mass axis, and negative ions are plotted below. These coatings produce distinctive spectra that can be differentiated from the others. Possible ion formulas based on product information and formulations are listed below in the text after each peak value. None of the ions observed have been determined to be molecular ions. For DuPont ChromaPremier[®] (B9708FM-1) Dark Mulberry Metal automotive paint (Fig. 1A), a number of prominent ions are present in the cation spectrum with mass 57⁺ (C₄H₉⁺) as the base peak. Generally, the hydrocarbon ion series m/z 29⁺, 43⁺, 57⁺, and 71⁺ are more abundant than the series m/z 27⁺, 41⁺, 55⁺, and 69⁺, which is indicative of the presence of saturated hydrocarbons moieties in the coating. This conclusion is based upon a favorable comparison between the relative ion intensities of the paint formulation with those of the docosane SIMS spectrum (35). Augmented ion abundance at m/z 41⁺ and 55⁺ (compared to docosane) may be due to C₂HO⁺ and C₃H₃O⁺ arising from polyurethane, which is a component of the DuPont ChromaPremier[®] automotive paints. The unique ion at m/z 130⁺

TABLE 1—Fingernail polish and paint samples analyzed by static SIMS.

Manufacturer	Product	Color	Manufacturer	Product	Color
DuPont	480S automotive	clear coat	Dupli-Color	Scratch-Fix Touch-Up	SF GM 388 bright red
DuPont	ChromaPremier automotive polyurethane	B9454FM C debonair red pearl metal	Dupli-Color	Scratch-Fix Touch-Up	SF GM 438 med. quasar metal
DuPont	ChromaPremier automotive polyurethane	B9522FH B wild orchid pearl metal	Dupli-Color	Scratch-Fix Touch-Up	SF GM 459 Light cloisonné metal
DuPont	ChromaPremier automotive polyurethane	B9605FM A thistle metal	Dupli-Color	Scratch-Fix Touch-Up	SF GM 460 med. cloisonné metal
DuPont	ChromaPremier automotive polyurethane	B9660FM F toreador red metal	Dupli-Color	Scratch-Fix Touch-Up	SF GM 461 med. adriatic metal
DuPont	ChromaPremier automotive polyurethane	B9708FM 1 dark mulberry metal	Dupli-Color	Scratch-Fix Touch-Up	SF GM 463 med. patriot red metal
DuPont	ChromaPremier automotive polyurethane	B9724FM 1 light toreador metal	Dupli-Color	Scratch-Fix Touch-Up	SF GM 479 cayan red metal
Dupont	Imron Automotive Polyurethane	Mustang NACA yellow green	Dupli-Color	Scratch-Fix Touch-Up	SF 125 Clear
Dupli-Color	Scratch-Fix Touch-Up	SF CC 341 garnet red	Maybelline	Revitalizing nail color	just your red 716
Dupli-Color	Scratch-Fix Touch-Up	SF CC 353 twilight blue metal	Wet'n'Wild	nail color nail polish	414 (red)
Dupli-Color	Scratch-Fix Touch-Up	SF CC 381 electric blue	Revlon	nail enamel nail polish	3994 love that red
Dupli-Color	Scratch-Fix Touch-Up	SF CC 382 radiant red	Cutex	color quick nail polish	rushing red 14
Dupli-Color	Scratch-Fix Touch-Up	SF CC 386 teal metal	L'Oreal	nail enamel nail polish	208 british red coat
Dupli-Color	Scratch-Fix Touch-Up	SF CC 392 spruce metal	Plasti-Kote	spray paint	fluorescent stoplight red
Dupli-Color	Scratch-Fix Touch-Up	SF CC 396 dark red pearl metal	Plasti-Kote	spray paint	harvest red
Dupli-Color	Scratch-Fix Touch-Up	SF FM 299 wild strawberry	EasyWay	spray paint	red primer
Dupli-Color	Scratch-Fix Touch-Up	SF FM 306 cardinal red	EasyWay	spray paint	swift red
Dupli-Color	Scratch-Fix Touch-Up	SF FM 317 ford red metal	Hank's Best	spray paint	chinese red
Dupli-Color	Scratch-Fix Touch-Up	SF FM 328 cayan metal	Hank's Best	spray paint	red oxide primer
Dupli-Color	Scratch-Fix Touch-Up	SF FM 340 royal blue	Rust-Oleum	spray paint	apple red gloss
Dupli-Color	Scratch-Fix Touch-Up	SF FM 345 pacific green	Rust-Oleum	spray paint	colonial red
Dupli-Color	Scratch-Fix Touch-Up	SF FM 387 dark blue metal	Rust-Oleum	spray paint	fluorescent red orange

is probably amine bearing ($C_8H_{20}N^+$), and may be derived from aliphatic polyamines, which are present as components in the formulation. Mass 91^+ ($C_7H_7^+$) is indicative of the presence of aromatic components. Mass 105^+ is attributed to $(C_6H_5)C_2H_4^+$ or possibly $(C_6H_5)CO^+$. The ions at m/z 147^+ , 151^+ , 163^+ , and 221^+ are consistent with $(C_6H_5)COOC_2H_2^+$, $(C_2H_4O)_3H_3O^+$, $(C_6H_5)(C_2H_3)COOCH_3^+$, and $HO_2CC_4H_8CO_2C_4H_8OH_2^+$, respectively. Mass 147^+ , and m/z 221^+ are also consistent with ions derived from polydimethylsiloxane for the series $(CH_3)_3Si(OSi(CH_3)_2)_n$ for $n = 1, 2$. Many of the other ions in the spectra could not be determined due to the complexity of the components present in the paint mixture. Generally, the anion spectrum is uninformative, although in this case acrylate (m/z 71^-) and propionate (m/z 87^-) can be observed in the spectrum.

For EasyWay Swift Red spray paint (Fig. 1B), the spectrum is dominated by ions derived from polydimethylsiloxane with ions at m/z 73^+ (base peak), 147^+ , and 221^+ that are consistent with the series $(CH_3)_3Si(OSi(CH_3)_2)_n$ for $n = 0, 1, 2$. PDMS is also responsible for ions at m/z 133^+ , 207^+ , and 281^+ which correspond to $(CH_3)_2HSi((OSi(CH_3)_2)_n)$ for $n = 1, 2, 3$. Few unique ions are seen in the anion spectrum, but masses at m/z 75^- , 149^- , and 223^- are present, and are consistent with PDMS-derived $CH_3SiO_2((CH_3)_2SiO)_n^-$ for $n = 0, 1, 2$.

Mass 91^+ ($C_7H_7^+$) is the base peak for the cation spectrum of L'Oreal® 208 British Red Coat nail enamel (Fig. 1C). Mass 91^+ was very abundant compared to the other fingernail polishes included in this study and is most likely derived from toluene sulfonamide/formaldehyde, as are m/z 155^+ ($C_6H_5CH_2SO_2^+$) and 184^+

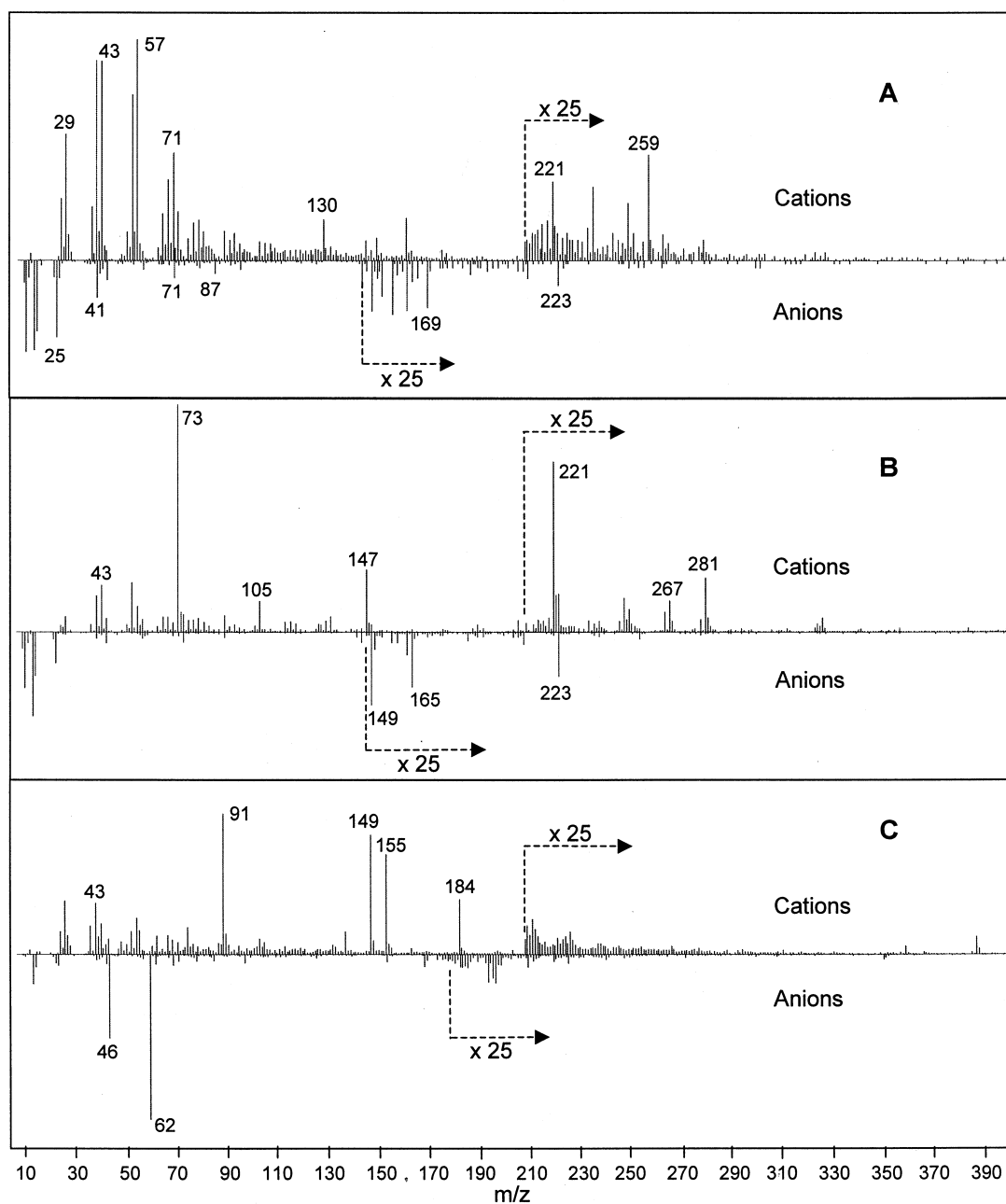


FIG. 1—Cation and anion SIMS spectra of coatings from different manufacturers. (A) DuPont ChromaPremier® B9708FM-1 Dark Mulberry Metal automotive paint; (B) EasyWay Swift Red spray paint; (C) L'Oreal® 208 British Red Coat nail polish. Cation spectra are plotted above the mass axis; anion spectra are plotted below.

($\text{HO}(\text{C}_6\text{H}_4)\text{NHSO}_2^+$). Mass 149^+ ($\text{C}_8\text{H}_5\text{O}_3^+$) was also prominent in the cation spectra and is usually attributed to phthalate derivatives. Typical saturated hydrocarbon isomers are seen at m/z 29^+ , 43^+ , and 57^+ . The ions at m/z 46^- and 62^- (NO_2^- and NO_3^-) are attributed to the nitrocellulose and dominate the anion spectrum; this is a fairly unique characteristic of this coating. A low abundance ion that is unique compared to other spectra, is observed at m/z 170^- ($(\text{C}_6\text{H}_5)\text{NHSO}_2\text{CH}_2^-$) and is attributed to toluene sulfonamide/formaldehyde as well.

SIMS Spectra of Coatings from a Single Product Line

In some cases, spectra were difficult to distinguish, particularly if they were derived from a single product line of a given manu-

facturer. For example, Fig. 2 shows a series of SIMS spectra of DuPont ChromaPremier® Debonair Red Pearl Metal (B9454FM-C), Wild Orchid Pearl Metal (B9522FH-B), and Light Toreador Metal (B9724FM-1) automotive paint. As with the spectra of DuPont ChromaPremier® (B9708FM-1) Dark Mulberry Metal automotive paint (Fig. 1A), the spectra in Fig. 2 are dominated by the hydrocarbon ion series m/z 27^+ , 29^+ , 41^+ , 43^+ , 55^+ , 57^+ , 69^+ , and 71^+ , with m/z 43^+ as the base peak for the three spectra. Relatively abundant ions are observed at m/z 130^+ and m/z 163^+ , along with the high mass ions at m/z 237^+ , 251^+ , and 259^+ . The ions at m/z 25^- (C_2H^-), 41^- (C_2OH^-), 42^- (CNO^-), and 59^- (CH_3COO^-) are observed in the anion spectrum along with acrylate (m/z 71^-) and propionate (m/z 87^-) ions. Generally, only differences in ion

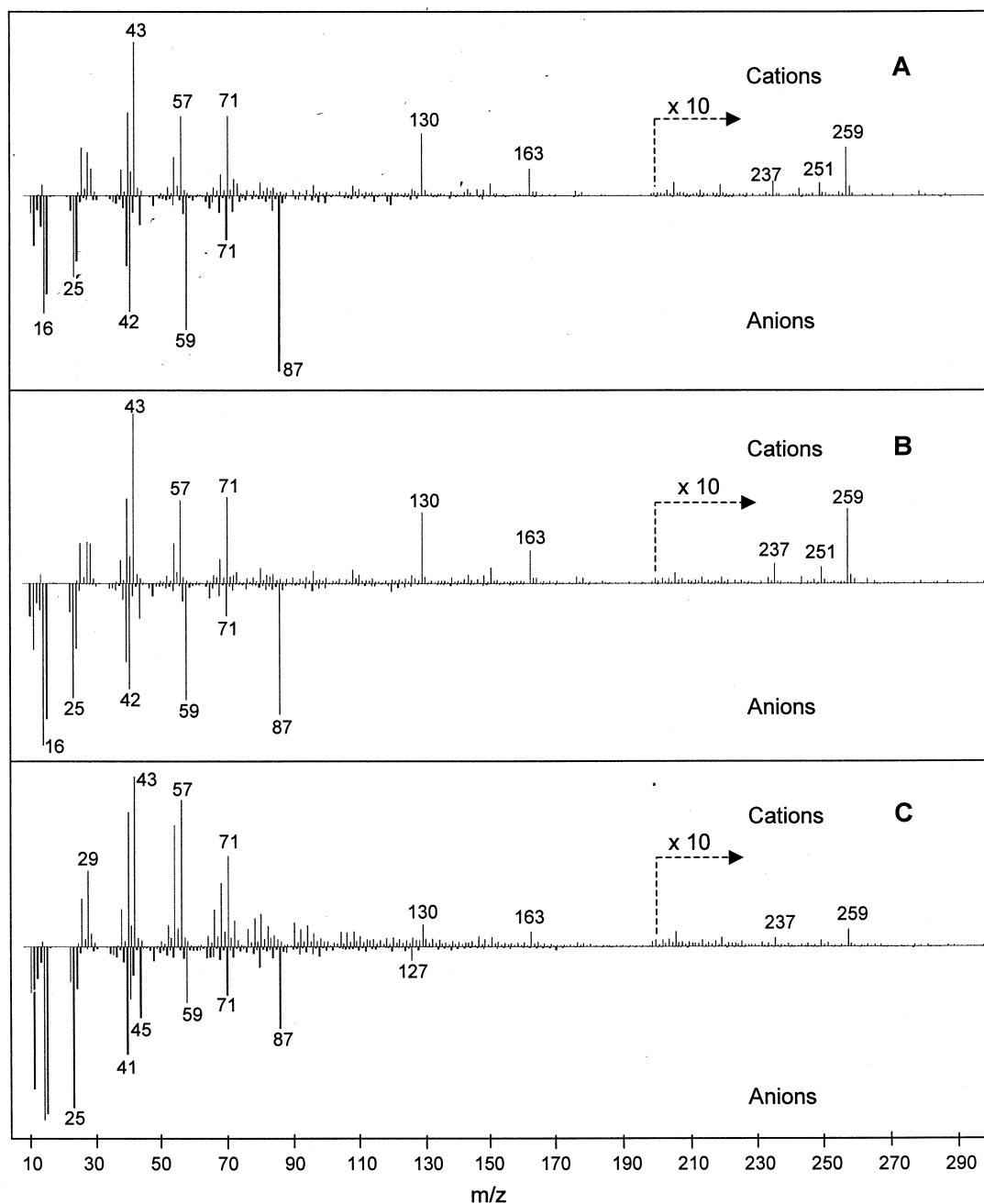


FIG. 2—Cation and anion SIMS spectra of DuPont ChromaPremier[®] automotive paints; (A) B9454FM-C Debonair Red Pearl Metal; (B) B9522FH-B Wild Orchid Pearl Metal; (C) B9724FM-1 Light Toreador Metal. Cation spectra are plotted above the mass axis; anion spectra are plotted below.

abundance are observed in the spectra, with the exception of the presence of m/z 127⁻ in the Light Toreador Metal (B9724FM-1) paint (Fig. 2C). The spectra are visually similar and difficult to differentiate, however the differences in the relative ion intensities could be significant in forensic comparisons provided the differences are shown to be highly reproducible when replicate analyses are conducted. Differentiation was also difficult in the PCA analysis presented below of the DuPont ChromaPremier[®] automotive paints (see Fig. 6), and was the reason that the paints were grouped together as a single paint product.

Spectral Consistency and Sample Alteration of a Single Sample after Multiple SIMS Analyses

A single coating sample of DuPont Imron Mustang NACA Yellow Green (nonmetallic polyurethane enamel) automotive paint was painted onto a SIMS sample target and analyzed by IR reflectance microspectroscopy and SIMS. The purpose for the sequential analyses was to determine the level of spectral variation caused by the SIMS analysis and to address the question as to whether valid or defensible IR spectral comparisons can be

achieved after SIMS analysis. The sample was initially analyzed by reflectance FT-IR and then sequentially analyzed by SIMS, reflectance FT-IR, and SIMS. Figure 3 shows a series of reflectance FT-IR spectra, obtained before and after quadrupole SIMS analysis. The estimated primary ion dose for each SIMS analysis was 2.2×10^{12} ions/cm². The FT-IR spectra represent a "snapshot" of the surface after the static SIMS analysis, and indicate that there are some minor changes in the IR spectra. This can be due to a number of factors. First, due to lack of visible surface landmarks, it was not possible to verify if the pre-SIMS and post-SIMS IR analyses were exactly in the same location. If the sample is heterogeneous, this

may account for variations in the IR spectra. Second, the effects of exposing the sample to a high vacuum environment were not evaluated. It is possible that enhanced desolvation, as sublimation or evaporation may occur. Third, the first few monolayers of sample surface are sputtered away during the SIMS process. This can alter the surface morphology of the sample and induce changes in the degree of specular reflectance contribution to the IR spectra. As seen in Fig. 3B, the spectral bands present in the initial FT-IR spectrum are still present after the SIMS analysis; however, there are minor differences. Absorbance in the C-H stretch region (2800–3100 cm⁻¹) has been reduced, possibly due to the cleavage of

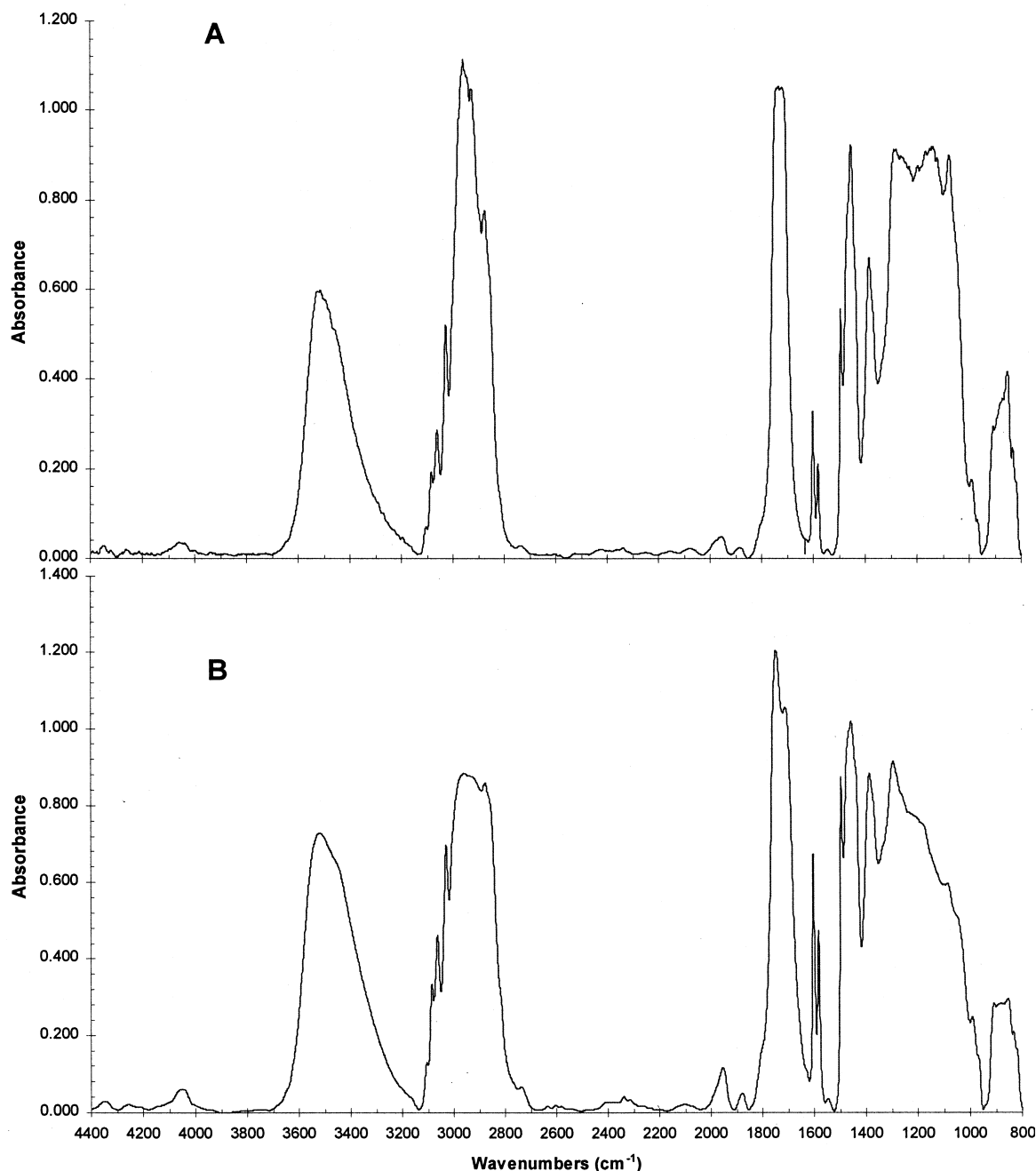


FIG. 3—FT-IR spectra of DuPont Imron® NACA Yellow Green automotive paint: (A) Prior to SIMS bombardment; (B) After SIMS analysis, primary ion dose of 2.2×10^{12} ions/cm².

alkyl groups from the aromatic or polymer surface. There is also an enhancement of the aromatic bands at 1875 cm^{-1} and 2000 cm^{-1} , which is consistent with reduction of aliphatic moieties. The fingerprint region (1400 cm^{-1} and 800 cm^{-1}) also showed negligible differences. The sample appeared to be more polished under the visible microscope after the initial SIMS analysis and spectral reflectance was increased by a factor of 10. The pre- and post-SIMS IR spectra do not indicate any significant changes in the sample. This would be consistent with the SIMS affect and IR sampling depth of penetration in the range of nanometers and micrometers, respectively.

The second SIMS spectrum showed little variation due to the initial SIMS analysis. Figure 4 shows two sets of cation/anion spectra, representing primary ion dose values of 2.2×10^{12} and 4.4×10^{12} ion cm^{-2} , obtained using the quadrupole SIMS instrumentation. Comparison of the spectra shows no significant difference in the SIMS spectra with the exception that the total ion abundance was reduced from 200 K counts in the cation spectra for the initial SIMS analysis to 140 K counts in the second SIMS analysis. The most likely reason for the reduced abundances is removal of surface species through ion bombardment. The removal of the surface species is also likely to be responsible

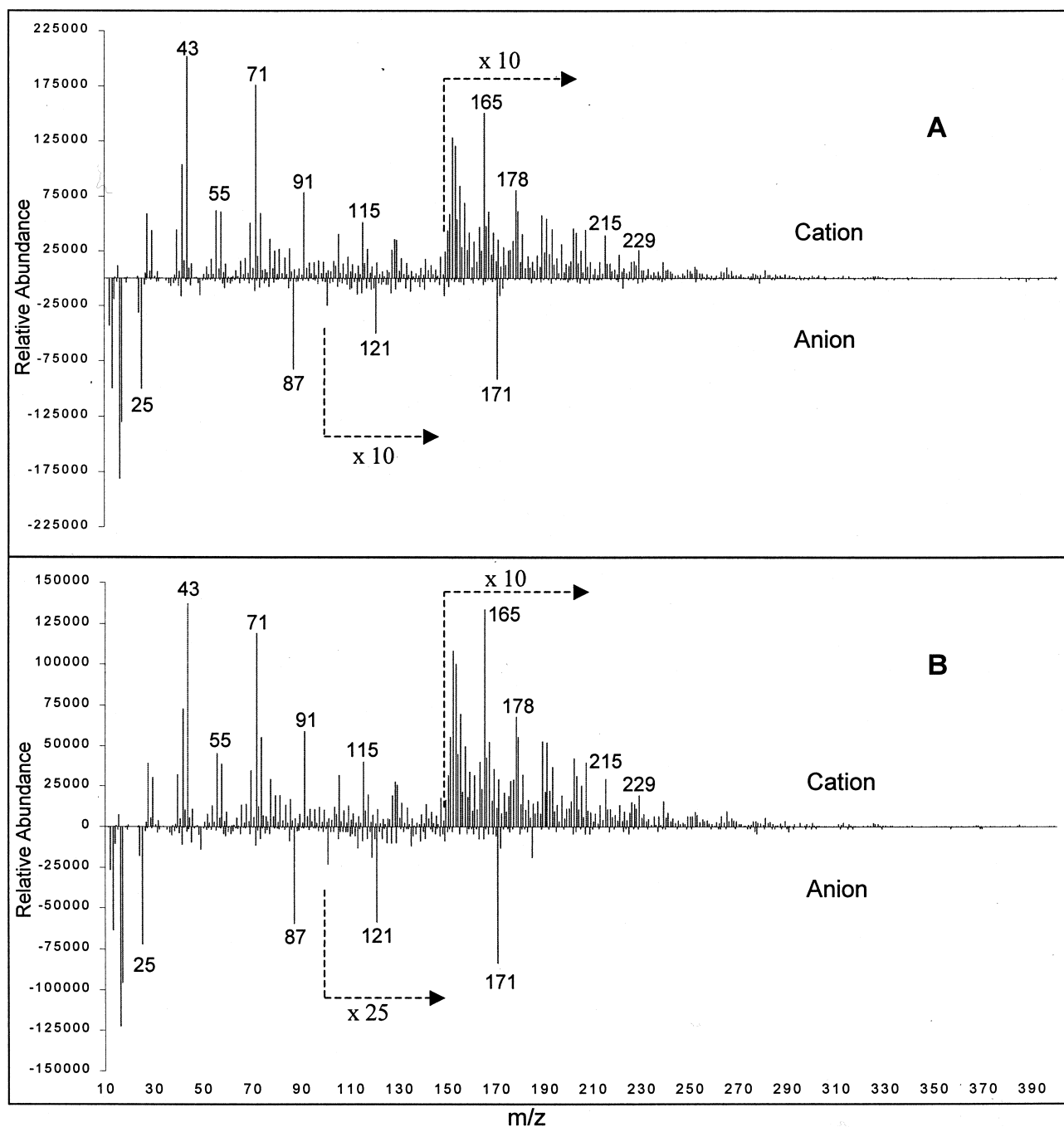


FIG. 4—Cation and anion SIMS spectra of DuPont Imron® NACA Yellow Green automotive paint. (A) Initial analysis, primary ion dose of 2.2×10^{12} ions/ cm^2 ; (B) Second analysis, primary ion dose of 4.4×10^{12} ions/ cm^2 . Cation spectra are plotted above the mass axis; anion spectra are plotted below.

for changes in the IR spectra, although the relative spectral abundances observed in the SIMS spectrum were not affected. While these experiments show that while SIMS is destructive to the top-most layer of the sample, the bulk of the sample is completely unaltered, and hence the sample may be used for subsequent analysis using other analytical techniques.

Statistical Approach to Spectral Identification

The static SIMS spectra of the coatings evaluated are distinctive and can generally be differentiated from each other. In most cases the coatings can be differentiated by manufacturer, and frequently to the specific product for the coatings tested. However, the spectral differences observed when comparing the DuPont ChromaPremier® automotive paints and Dupli-Color Scratch-Fix® Touch-Up paints were not as significant, and therefore made differentiation difficult. Other differentiation problems were also encountered due to the large number of spectra generated. To improve differentiation, multivariate analysis methods (38) were applied. Multivariate analysis methods commonly used to determine analyte concentrations in overlapped spectra include classical least squares (CLS) (39), partial least squares (PLS) (40), principal component analysis or regression (PCA or PCR) (41), and occasionally, neural networks (NN) (42).

CLS can be used quite effectively in relatively simple systems where all components that will contribute to the spectrum are known. Calibration for CLS can be as simple as having a pure analyte spectrum at a single known concentration for every component in the system expected to contribute to the spectrum. For this research each coating was assumed to be pure (e.g., free of aberrations due to contamination), and set to a concentration of 1. The key is that every contributor to the spectrum must be known; anything not found in the calibration set will cause large errors. Some examples of things that cause problems with the use of CLS include interfering chemical species, odd-shaped backgrounds, or concentrations outside the linear range modeled.

Spectral decomposition methods like PLS and PCR are better able to accommodate many of the problems that limit CLS. PLS is different from PCR in that the concentration information is included in the spectral decomposition as a one-step process that has the effect of weighting the spectra with the highest analyte concentrations. Because of the weighting, the resulting spectral factors are more closely related to the analyte spectrum and are therefore frequently considerably different than those calculated in PCR. Again, all spectra were assumed to have a concentration of 1 for this work. The resulting advantages are similar, however. Both PLS and PCR can be used for very complex mixtures since for the training set only the concentrations of the analyte of interest are required a priori. PLS and PCR can model some nonlinearity, and hence are also less affected by unknown components or other spectral aberrations than is CLS. The interferences, nonlinearities, abnormal backgrounds, etc., must still be included in the calibration set; however, exact knowledge of their source, identity or magnitude is not necessary.

In the following sections, three multivariate statistical approaches are discussed. The reason for this methodology is that finding similarities and differences in data is not necessarily a straightforward approach without distinctive insight into the problem. Spectral identification of unknown coatings was initially attempted using all of the sample coating types as individual components and a PLS calibration; however, poor results were obtained using this approach. Using PCA score plots, specific spectra were

grouped together to overcome the problems encountered in the initial PLS analysis. Correlation spectra were also investigated as a means of establishing spectral differences and identifying unique ions to enhance the differentiation process. The application of an optimized PLS to the identification of coatings from mass spectra was achieved using two criteria to define the results.

Classification of Coatings Using Multivariate Statistical Analysis

Multivariate analysis methods were required due to the large number of complex SIMS spectra acquired (greater than 300 total spectra). Spectra were normalized prior to multivariate analysis. Anion spectra were normalized by dividing the ion intensity at each point by the mean ion intensity in the mass range of m/z 26.5⁻ to 300⁻. Cation spectra were normalized by dividing the ion intensity at each point in the cation spectrum by the mean ion intensity in the mass range of m/z 44.5⁺ to 54.5⁺, m/z 55.5⁺ to 72.5⁺, and m/z 73.5⁺ to 300⁺. The excluded mass regions were selected to exclude high abundance, ubiquitous ions, which would dominate the normalization, particularly on sample spectra with low signal-to-noise ratios. The resulting normalized negative and positive ion spectra were then combined to make one spectrum where the negative ion portion of the new spectrum was assigned negative mass units (see, for example, Fig. 8). A matrix consisting of the “number of spectra” by “number of components” was constructed, in which each of the spectra in the calibration set was assigned a value to identify it as one of the components. For unknown spectra, a positive identification was indicated by a value of 0.95 and a negative identification was assigned a value of -0.95. In the final PLS calibration there were 232 spectra and 19 coatings classes.

Because of the large number of calibration samples and potential components, using PLS or PCR factors and scores to verify groupings is extremely difficult. Therefore, spectral identification of unknown coatings was attempted using all of the sample coating types as individual components and a PLS calibration. However, even when using this approach, poor results were obtained. For many of the coatings, it was suspected that many of the coating formulations might be similar, particularly if they came from a single product line of a manufacturer. Only for one Revlon sample was the spectral residual enough to indicate that the results were suspect.

The spectral residual is calculated by reconstructing the sample spectrum from the PLS model and subtracting it from the actual spectrum to create a “residual spectrum.” Each point of this spectrum is then squared and these values are summed to create the spectral residual (i.e., spectral residual = SUM (reconstructed spectrum-actual spectrum)²). The sample spectrum residual is compared to the average spectral residual from the calculation set via an F-test to determine outliers. High sample spectral residuals may result either from excessive noise in the sample spectrum or because the sample spectrum does not match well with any of the spectra in the calibration set. Therefore, the defined factors are not adequate to describe this spectrum. For this particular Revlon sample, the signal-to-noise was good, therefore it appears that the spectrum was not consistent with the other Revlon spectra or any of the other coating spectra. Generally, any sample with a high spectral residual should be examined to guard against misidentification and to determine if the spectrum may truly be an unknown.

Grouping of Data Using PCA

To test the concern of whether the coating formulations might be similar and to assess analytical reproducibility, the calibration set was separated into groups, e.g., all nail polishes, all coatings from

Dupont, etc. PCA was then used to generate score plots which were visually examined for clustering. Figure 5 is such a score plot for the five nail polishes. Because of the complexity of the formulations and the resulting mass spectra, a total of 11 factors are necessary to describe the system; however, factors 1 through 3 contain the most information. Individual spectra within the L'Oreal® 208 British Red Coat nail enamel and Cutex Rushing Red 14 nail polish groups, collected over an 8-to-12-month period, were reproducibly clustered together, which demonstrated the reproducibility of the static SIMS spectra. Each nail polish has a grouping that is reasonably well separated from the other polishes indicating that they indeed do have unique spectral characteristics. There were two potential outliers that correlate to Cutex in this plot. For the L'Oreal® spectrum, poor correlation was likely due to an extremely

poor signal-to-noise ratio. An incorrectly correlated Wet'n'Wild 414 Red nail polish spectrum was found to have peak ratios that did not match well with all of the other Wet'n'Wild spectra. Both spectra were dropped from the final calibration set. All of the nail polishes were treated as unique coatings in the final PLS1 application.

Figure 6 is a similar score plot for all of the DuPont coatings evaluated. This plot shows a general trend in the score plots for this group of spectra. Dupont 480 Clear Coat and Imron Mustang NACA Yellow Green appear to be independent groups that are significantly different from the other Dupont automotive coatings. Of the other coatings from Dupont, the DuPont ChromaPremier® B9454FM-C Debonair Red Pearl, B9522FH-B Wild Orchid Pearl and B9605FM-A Thistle Metal automotive paints appear to be indistinguishable from each other. Again, these spectra were col-

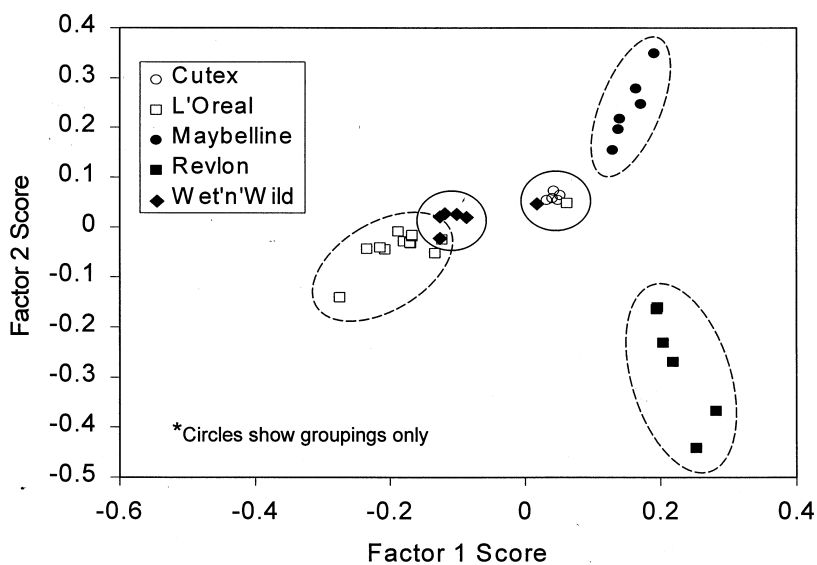


FIG. 5—Score plot of factors 1 and 2 from a Principal Component Analysis (PCA) of nail polishes.

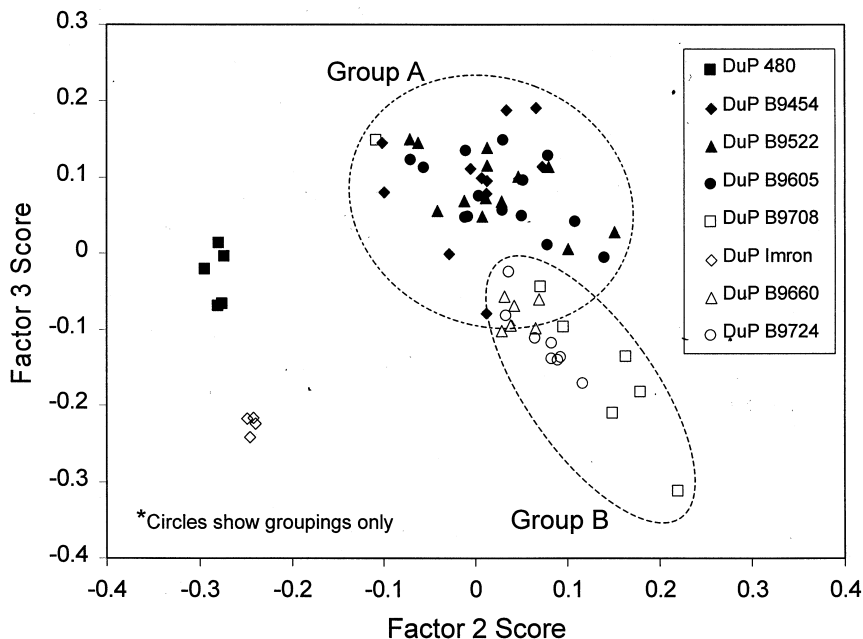


FIG. 6—Score plot of factors 2 and 3 from the Principal Component Analysis (PCA) of all of the DuPont coatings.

lected over several months within each group, indicating that the reproducibility is good. Because these coatings appeared to be nearly identical, they were grouped together and will hereafter be referred to as DuPont Group A. DuPont ChromaPremier[®] automotive paints B9708FM-1 Dark Mulberry Metal, B9660FM-F Toreador Red Metal and B9724FM-1 Light Toreador Metal also appear to be very similar to each other, but different from Group A. These coatings were therefore grouped together and will hereafter be referred to as DuPont Group B. When reviewing the component formulations for all the DuPont ChromaPremier[®] automotive paints analyzed, three components (the binder, balancer, and flop control agent) make up 44% to 64% by weight of each paint mixture. The remaining components were generally the colorants and aluminum metal flake, therefore it is understandable that these coatings appeared to be nearly identical.

Similar analysis from the score plots of the relatively large group of Dupli-Color Scratch-Fix[®] Touch-Up paints indicated that the Dupli-Color paints were all very similar. The Dupli-Color paints were subsequently grouped together. No obvious groupings could be made with the Rust-Oleum (Apple Gloss Red, Colonial Red, or Fluorescent Red Orange), Plasti-Kote (Fluorescent Stoplight Red, or Harvest Red), EasyWay (Red Primer or Swift Red) or Hank's Best (Chinese Red or Red Oxide Primer) spray paints, so they were left as individual coatings. The PCA score plots confirmed that a variety of coatings from a specific manufacturer (i.e., DuPont ChromaPremier[®] automotive paints and Dupli-Color Scratch-Fix[®] Touch-Up paints) generally clustered together due to the similarity of the spectra. The PCA score plots also demon-

strated that the nail polishes and spray paints have groupings that are reasonably well separated from the other coating materials, indicating that they indeed do have unique spectral characteristics, which are highly reproducible.

Correlation Spectra

Correlation spectra highlight spectral differences and identify ions that are unique relative to the spectral database. From correlation information, target ions may possibly be selected to enhance identification, possibly through MS² analysis. The correlation spectrum is calculated using the ion intensity and "concentration" at every point in a given spectrum. The entire calibration set was used for this calculation. The most unique ions for a particular coating, compared to all of the other coatings in the data set, will have the highest correlation. Figure 7 is an example of an average L'Oreal[®] nail polish spectrum and a correlation spectrum L'Oreal[®] nail polish. In the negative ion portion of the average spectrum it is interesting to note that the largest peaks are due to nitrate and nitrite ions (m/z 46⁻ and 62⁻), however, these peaks do not appear in the correlation spectrum at all. Instead, lower abundance peaks at m/z 170⁻, 155⁻, and 64⁻ are the most prevalent in the negative ion correlation spectrum. The ion at m/z 149⁺ was a prominent ion in the positive ion spectrum but does not correlate well, indicating that it is not very unique.

One should keep in mind, however, that even though masses with significant correlations may not be present in the correlation spectrum, good working calibrations can be obtained when wide

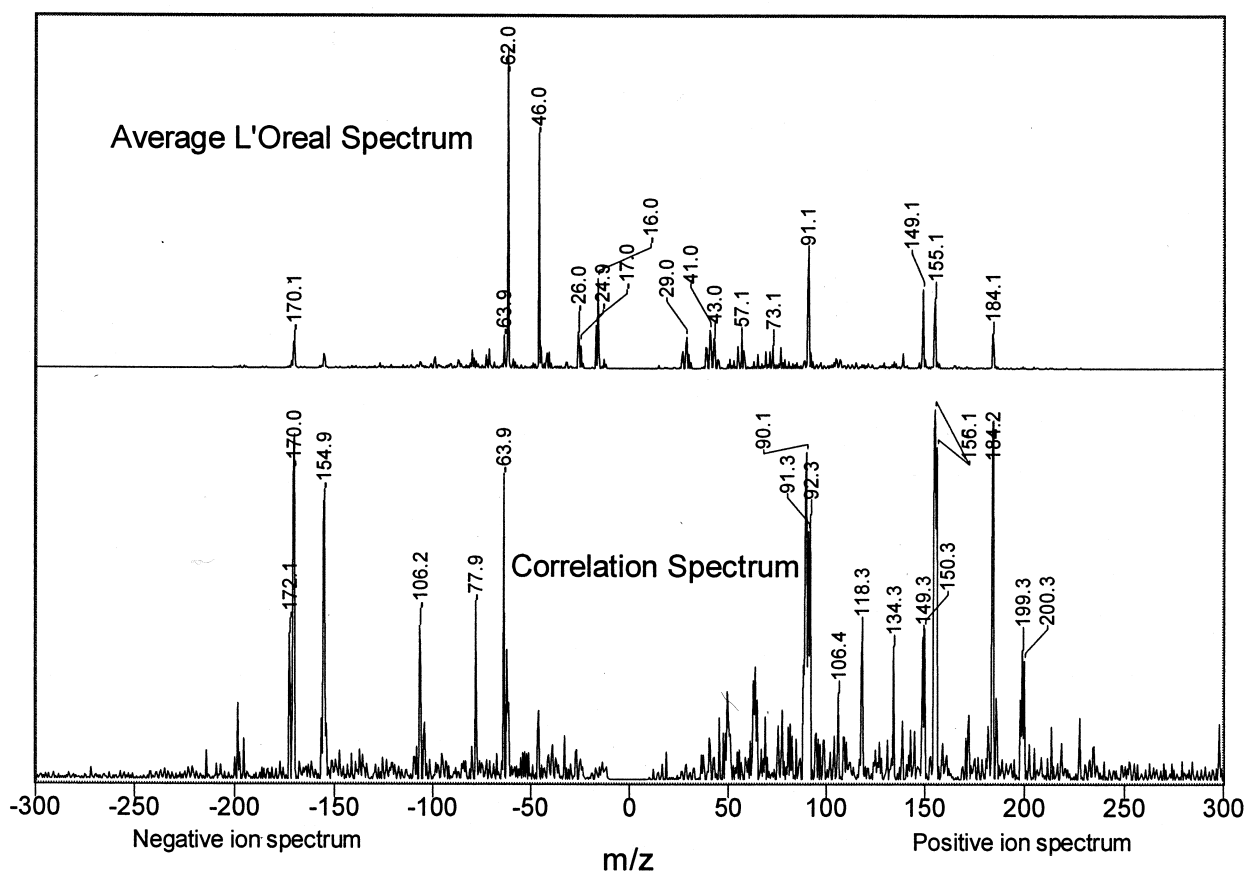


FIG. 7—Average L'Oreal nail polish spectrum compared with the correlation spectrum.

regions of the spectrum are used. This is because in many cases, it is the ion pattern that may be unique to the coating and not necessarily an individual ion or group of ions. In fact, just because some ions exist with high reasonability (e.g., high correlation between intensity and concentration) they may not provide results as good as if the entire spectrum is used. For example, Fig. 8 shows the correlation spectrum and corresponding normalized SIMS spectrum for the Wet'n'Wild nail polish. Relatively good correlation is observed at m/z 149⁺; this ion and several other masses in the positive ion spectrum seem to stand out as possible ions that may create a unique set for determining Wet'n'Wild. However, several combinations of these masses or selected spectral regions failed to produce a PLS1 calibration that could outperform the use of the entire combined negative and positive ion spectrum. Only for one coating (EasyWay Red Primer) were the correlations relatively nondescript. The lack of truly unique masses may result in misidentifications or questionable identifications.

Partial Least-Squares Analysis

The full calibration used to identify product spectra in an independent verification set was made using the PLS1 algorithm to model each component from a set of 232 spectra. The advantage of this algorithm is that each component can have an optimized set of factors as opposed to the PLS2 or PCR algorithms, which utilize a common number of factors. The analysis was checked with a set of 66 independent spectra (stand-alone sample spectra, which were not included in the calibration set) of the individual coatings.

Table 2 lists the results from the analysis of 66 independent spectra using the result of 0 as a decision point, with positive results >0,

and negative results <0. Sensitivity is defined as $TP/(TP+FN)*100$ where TP and FN denote the number of true positive and false negative results, respectively (43). For this application, sensitivity is a measure of how well the analysis performs in truly identifying the components in the coating spectra of interest that are actually present. Specificity is defined as $TN = TN/(TN+FP)*100$ where TN and FP denote the number of true negative and false positive results, respectively. Specificity is a measure of how well the PLS models discriminate against components not in the spectrum.

Only five misidentifications occurred in this analysis, two false positives and three false negatives. Two of the false positives and two of the false negatives are attributed to the identification of L'Oreal® 208 British Red Coat nail polish as DuPont Group A, and EasyWay Red Primer spray paint as Hank's Best Red Oxide Primer spray paint. When comparing the spectra of the DuPont ChromaPremier® automotive paints (Fig. 1A and Fig. 2) to that of the L'Oreal® 208 British Red Coat (Fig. 1C) the spectra are visibly different, therefore the misidentification must come from another source, perhaps mislabeled data files. The fifth misidentification was a false negative for a single Wet'n'Wild 414 Red nail polish sample. Overall, the model appears to be more than 90% effective in identifying the spectrum of a particular coating and nearly 100% effective at telling which coating components represented in the PLS models are not present in a spectrum.

As presented in Table 2, the application of PLS to the identification of coatings from mass spectra appears to result in a simple yes/no answer. In practice, this may cause a problem because it does not give an indication of how good the identification is. A better method may be to define true and false positive results as those

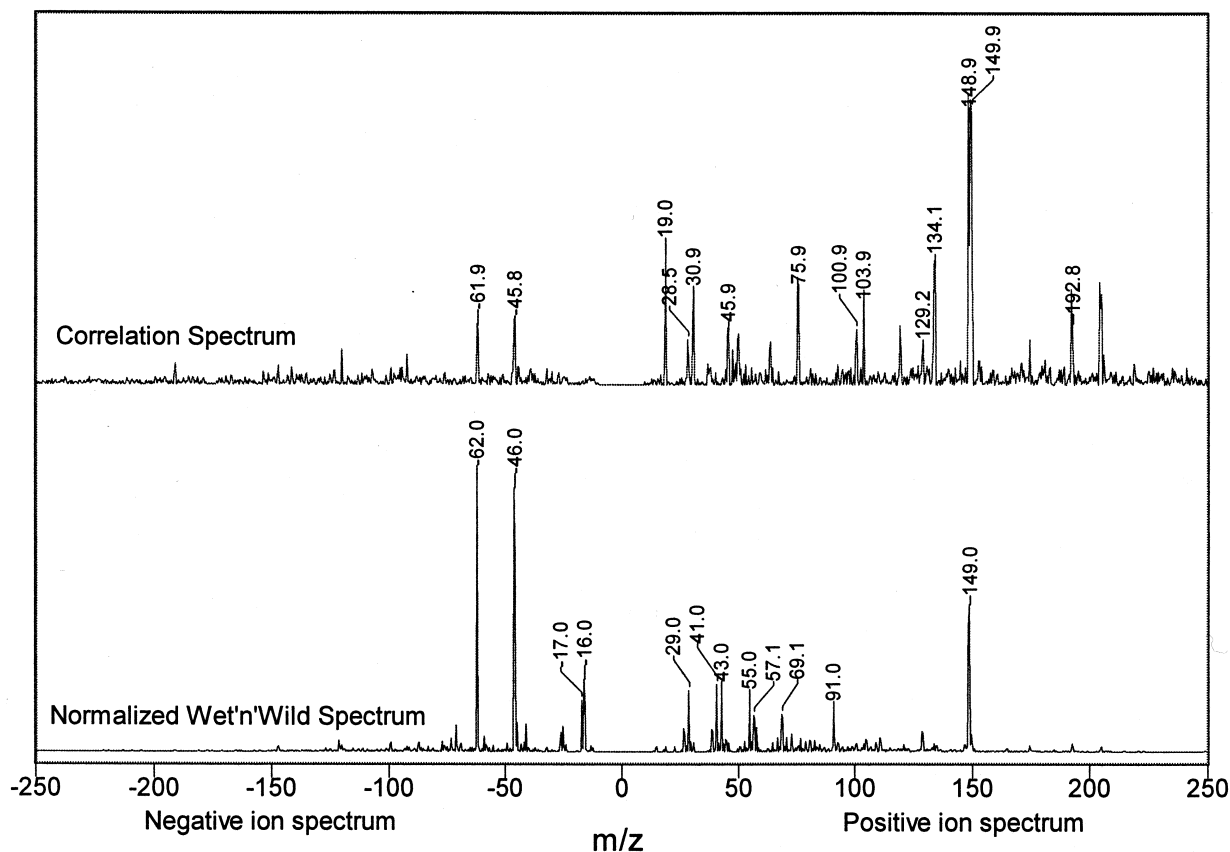


FIG. 8—Correlation and normalized positive and negative ion spectra of Wet'n'Wild.

TABLE 2—Results from the Partial Least Squares (PLS1) identification analysis of 66 independent spectra using a value of 0 as a decision point; i.e., >0 indicates a positive identification.

Coating	True Positive	True Negative	False Positive	False Negative	% Sensitivity	% Specificity
Cutex	4	62	0	0	100	100
DuPont 480S	2	64	0	0	100	100
DuPont-GrpA	7	58	1	0	100	98
Dupont GrpB	8	58	0	0	100	100
DuPont Imron	0	66	0	0	NA	100
EasyW Primer	2	63	0	1	67	100
EasyW SwftR	4	62	0	0	100	100
Hank's ChinaR	3	63	0	0	100	100
Hank's PrimeR	2	63	1	0	100	98
L'Oreal BRC	2	64	0	0	100	100
Maybelline	2	64	0	0	100	100
Plasti-K FSR	4	62	0	0	100	100
Plasti-k HR	2	64	0	0	100	100
Rust-O AR	2	64	0	0	100	100
Rust-O ColR	2	64	0	0	100	100
Rust-O FRO	2	64	0	0	100	100
Revlon LTR	3	62	0	1	75	100
Dupli-C Group	9	57	0	0	100	100
Wet'n'Wild	3	62	0	1	75	100
Total	63	1186	2	3	95	100

TABLE 3—Results from the Partial Least Squares (PLS1) identification analysis of 66 independent spectra using values of 0.3 and -0.3 as decision points for positive and negative results, respectively.

Coating	True Positive ≥ 0.3	True Negative ≤ -0.3	False Positive ≥ 0.3	False Negative ≤ -0.3	?False Positive $-0.3 < FP < 0.3$?False Negative $-0.3 < FN < 0.3$	Sensitivity %	Specificity %
Cutex	3	62	0	0	0	1	75	100
DuPont 480S	2	64	0	0	0	0	100	100
DuPont GrpA	7	58	0	0	1	0	100	98
DuPont GrpB	8	58	0	0	0	0	100	100
DuPont Imron	0	66	0	0	0	0	NA	100
EasyW Primer	1	63	0	0	0	2	33	100
EasyW SwftR	4	62	0	0	0	0	100	100
Hank's ChinaR	3	61	0	0	2	0	100	97
Hank's PrimeR	0	62	0	0	2	2	0	97
L'Oreal BRC	2	64	0	0	0	0	100	100
Maybelline	2	63	0	0	1	0	100	98
Plasti-K FSR	3	62	0	0	0	1	75	100
Plasti-k HR	2	64	0	0	0	0	100	100
Rust-O AR	2	63	0	0	1	0	100	98
Rust-O ColR	2	64	0	0	0	0	100	100
Rust-O FRO	2	64	0	0	0	0	100	100
Revlon LTR	3	62	0	0	0	1	75	100
Dupli-C Group	8	57	0	0	0	1	89	100
Wet'n'Wild	1	62	0	1	0	2	25	100
Total	55	1181	0	1	7	10	83	99

≥ 0.3 , true and false negative results as those ≤ -0.3 , and all those between -0.3 and 0.3 as uncertain identifications. Results falling within the region of uncertain identification would require additional verification. Table 3 lists the results shown in Table 2 using these criteria. While the numbers of false positives and negatives have dropped to only one, there are 17 results that fall into the region of uncertain identification. Sensitivity is still $>80\%$ and the specificity is better than 95% in almost every case.

The reasons for the misidentifications and questionable identifications are likely related to the variability contained within and between the SIMS spectra of the calibration and verification sets, and the lack of truly unique identifying masses for some coatings. The

variability in the calibration and verification data sets sometimes arises from poor signal-to-noise ratios but is primarily due to ubiquitous ions that may also be a major part of the spectrum of a particular coating. Both of these factors can have a dramatic effect on the procedure used to normalize the spectrum. The variability in the intensity of the ubiquitous ions will skew the overall shape of the resulting mass spectrum in general. This may also significantly alter the intensity of critical selected masses during normalization, causing poor signal-to-noise ratios to amplify the noise during the normalization. Figures 7 and 8 also indicate that even though many of the coatings can be grouped quite nicely by their mass spectra, there are also subtle differences between many of the groups, and slight

variations in the spectra may increase the difficulty of getting a precise match. There are two possible ways to improve the calibration overall. The first would be to optimize the normalization of the spectrum, possibly by even having unique normalization criteria for each coating. The second would be to optimize the masses or mass regions used in the calibration for each coating. In this way, spectral interferences and regions of the spectrum that contribute primarily to noise can be avoided. This methodology has worked well for the determination of over 30 compounds from a single infrared spectrum, but its implementation can be time consuming (44).

The fact that the spectra for both the calibration and independent verification sets were collected over a period of several months may also offer another possible explanation for the misidentifications and questionable identifications. Two SIMS spectra from a weathered sample of Hank's Prime Red were included in the verification set. The model seems to have correctly identified this coating, however, the magnitudes of the results fall into the region of uncertainty. Two spectra of Revlon nail polish from the verification set produced high spectral aberrations, indicating that something in the spectra was significantly different from anything modeled by the calibration set. Indeed, significant ions were observed at m/z 43⁻, 111⁻, 113⁻, 115⁻, 159⁻, and 100⁺ that were not in any other spectrum of nail polish (Revlon or otherwise). It is not clear what caused the appearance of these ions in the spectra, however, the two suspect spectra were recorded in a serial fashion and these ions were much more prevalent in the first spectrum, which suggests the possibility of surface contamination. In fact, m/z 100⁺ has been attributed to cyclohexylamine, an atmospheric surface contaminant occasionally present in our laboratory (31).

Conclusion

Static quadrupole SIMS has been shown to be applicable to the forensic characterization and differentiation of coating materials. High signal-to-noise spectra containing abundant spectral information were obtained in less than 5 min. The SIMS instrumentation proved to be easy to operate and provided good sensitivity.

The reproducibility of the coating spectra and the static SIMS technique has been demonstrated. The reproducibility has been established through evaluation of coating spectra using multiple samples, multiple analysis of the same sample and collection of spectra over an 8-to-12-month period. This is highlighted via the PCA score plots for the fingernail polishes and DuPont automotive paints. The fingernail polishes emphasize this the best, as the PCA results were reasonably grouped and reasonably separated from the other polishes, indicating that they indeed do have consistent and unique spectral characteristics. This is also substantiated through the sequential SIMS analysis of a single coating sample of DuPont Imron Mustang NACA Yellow Green automotive paint. Some spectral variation in the IR spectra after SIMS analysis was observed; however, fundamentally the spectra were equivalent, which would indicate that static SIMS and IR could be used sequentially. Nevertheless, additional studies to determine the specific basis for the spectral variation of the IR spectra would be required.

The application of chemometric techniques for the classification of coatings from their SIMS spectra has been demonstrated. Principal component analysis (PCA) showed distinct spectral differences between most spectral groups, although limited correlation overlap was observed in some cases. Plotting the correlation spectra readily highlighted salient spectral differences. The most unique ions for a particular coating were not routinely the largest peaks in

the average spectrum. Partial Least Squares (PLS) permitted unknowns to be correctly grouped with few exceptions. The sensitivity with which coatings can be positively identified is greater than 95% and the specificity for a particular coating is essentially 100%. The methodology appears to be satisfactory; however, the calibration sets used were limited and consequently the multivariate approach was restricted. Improved results can most likely be obtained by refining calibration sets. Only for one Revlon sample was the spectral residual enough to indicate that the results were suspect and only for one coating material (EasyWay Red Primer) were the correlations relatively nondescript.

Acknowledgments

The authors wish to thank John Jolley for performing the IR analyses and the SIMS Research Group at the Idaho National Engineering and Environmental Laboratory for their collaboration and support.

References

1. Fong W. Analytical methods for developing fibers as forensic science proof: A review with comments. *J Forensic Sci* 1989;34(2):295-311.
2. Allen TJ. The examination of thin sections of coloured paints by light microscopy. *Forensic Sci Int* 1992;57(1):5-16.
3. Hammer PS. Pigment analysis in the forensic examination of paints. III. Guide to motor vehicle paint examination by transmitted light microscopy. *J Forensic Sci* 1982;22(2):187-92.
4. Norwicki J, Patten R. Examination of US automotive paints. I. Make and model determination of hit-and-run vehicles by reflectance microspectrophotometry. *J Forensic Sci* 1986;31(2):464-70.
5. Cousins DR, Plantoni CR, Russell LW. Use of microspectrophotometry for identification of pigments in small paint samples. *Forensic Sci Int* 1984;24(3):183-96.
6. Allen TJ. Paint sample presentation for Fourier transform infrared microscopy. *Vib Spectros* 1992;3(3):217-37.
7. Bartick EG, Tungal MW, Reffer JA. A new approach to forensic analysis with infrared microscopy: internal reflection spectroscopy. *Anal Chem Acta* 1994;28(1):35-42.
8. Burke P, Curry CJ, Davies LM, Cousins DR. Comparison of pyrolysis/mass spectrometry, pyrolysis/gas chromatography and infrared spectroscopy for the analysis of paint resins. *Forensic Sci Int* 1985;28(3-4):201-19.
9. Suzuki EM, Marshall WP. Infrared spectra of U.S. automotive original topcoats (1974-1989): IV. Identification of some organic pigments used in red and brown monocoats—quinacridones. *J Forensic Sci* 1998;43(3):514-42.
10. Tungal MW, Bartick G, Montaser A. Analysis of single polymer fibers by Fourier transform infrared microscopy: the results of case studies. *J Forensic Sci* 1991;36(4):1027-43.
11. Lang PL, Katon JE, O'Keefe JF, Schiering DW. The identification of fibers by infrared and Raman microspectroscopy. *Microchem J* 1986;34:319-31.
12. Keen IP, White GW, Frederick PM. Characterization of fibers by Raman microprobe spectroscopy. *J Forensic Sci* 1998;43(1):82-9.
13. Koenig JL. Spectroscopic characterization of polymers. *Anal Chem* 1987;59:1141A-55A.
14. McMinn DG, Carlson TL, Munson TO. Pyrolysis capillary gas chromatography/mass spectrometry for analysis of automotive paints. *J Forensic Sci* 1985;30(4):1064-73.
15. Challinor JM. Pyrolysis gas chromatography: some forensic applications. *Chem Aust* 1990;57(4):90-2.
16. Sansom PC. Applications of chromatography to the analysis of paints. *Anal Proc* 1981;18(9):393-4.
17. Fuller NA. Analysis of thin-layer chromatograms of paints pigments and dyes by direct microspectrophotometry. *Forensic Sci Int* 1985;27(3):189-204.
18. Yinin J, Saar J. Analysis of dyes extracted from textile fibers by thermospray high-performance liquid chromatography-mass spectrometry. *J Chrom* 1991;586:73-84.
19. Cousins DR. Developments in paint analysis for forensic purposes. *Paint Col J* 1988;178(4225):824-5.

20. Goebel R, Stoecklein W. The use of electron microscopic methods for the characterization of paints in forensic science. *Scanning Microscop* 1987;1(3):1007–15.
21. Beam TL, Willis WV. Analysis protocol for discrimination of automotive paints by SEM-EDXA using beam alignment by current centering. *J Forensic Sci* 1990;35(5):1055–63.
22. Walzak MJ, Davidson R, Biesinger M. The use of XPS, FTIR, SEM/EDX, contact angle, and AFM in the characterization of coatings. *J Mat Eng Performance* 1998;7:317–23.
23. Castle DA. Pigment analysis in the forensic examination of paints. II. Analysis of motor vehicle paint pigments by chemical tests. *J Forensic Sci* 1982;22(2):179–86.
24. Thorton JI, Kraus S, Lerner B, Kahane D. Solubility characterization of automotive paints. *J Forensic Sci* 1983;28(4):1004–6.
25. Delmore JE, Appelhans AD, Peterson ES. Tube ion source for the study of chemical effects in surface ionization. *Int J Mass Spectrom Ion Proc* 1991;108:179–87.
26. Ingram JC, Appelhans AD, Groenewold GS. Ion trap SIMS analysis of pinacolyl methylphosphonic acid on soil. *Int J Mass Spectrom Ion Proc* 1998;175:253–62.
27. Ingram JC, Groenewold GS, Appelhans AD, Delmore JE, Olson JE, Miller DL. Direct surface analysis of pesticides on soil, leaves, grass and stainless steel by static secondary ion mass spectrometry. *Environ Sci Technol* 1997;31:402–8.
28. Ingram JC, Groenewold GS, Appelhans AD, Dahl DA, Delmore JE. Detection limit and surface coverage determination for tributyl phosphate on soils by static SIMS. *Anal Chem* 1996;68:1309–16.
29. Groenewold GS, Appelhans AD, Ingram JC, Gresham GL, Delmore JE, Dahl DA. Detection of 2-chloroethylethyl sulfide on soil particles using ion trap secondary ion mass spectrometry. *Talanta* 1998;47:981–6.
30. Groenewold GS, Ingram JC, Delmore JE, Appelhans AD, Dahl DA. Detection of 2-chloroethyl ethyl sulfide and sulfonium ion degradation products on environmental surfaces using static SIMS. *Environ Sci Technol* 1995;29:2107–11.
31. Groenewold GS, Ingram JC, Gianotto AK, Appelhans AD, Delmore JE. Static secondary ion mass spectrometry detection of cyclohexylamine on soil surfaces exposed to laboratory air. *J Am Soc Mass Spectrom* 1996;7:168–72.
32. Groenewold GS, Appelhans AD, Ingram JC. Characterization of bis(alkylamine)mercury cations from mercury nitrate surfaces using an ion trap SIMS. *J Amer Soc Mass Spectrom* 1998;9:35–41.
33. Groenewold GS, Ingram JC, Appelhans AD, Delmore JE. Static SIMS detection of gold cyanide complexes on carbon using crown ethers enhancement. *Anal Chem* 1995;67:1987–91.
34. Briggs D, Brown A, Vickerman JC. *Handbook of static SIMS*. Great Britain: John Wiley & Sons, 1989.
35. Newman JG, Carlson BC, Michael RS, Moulder F. *Static SIMS handbook of polymer analysis*. Perkin-Elmer Corp, 1991.
36. Briggs D, Hearn MJ. Interaction of ion beams with polymers, with particular reference to SIMS. *Vacuum* 1986;36:1005–10.
37. Appelhans AD, Dahl DA, Delmore JE. Neutralization of sample charging in secondary ion mass spectrometry via pulsed extraction field. *Anal Chem* 1990;62:1679–86.
38. Brown SD. Chemical systems under indirect observation: latent properties and chemometrics. *Appl Spectro* 1995;49:14A–31A.
39. Haaland DM, Easterling RG, Vopicka DA. Multivariate least-squares methods applied to quantitative spectral analysis of multicomponent samples. *Appl Spectro* 1985;39:73–84.
40. Haaland DM, Thomas EV. Partial least-squares methods for spectral analysis. 1. Relation to other quantitative calibration methods and extraction of qualitative information. *Anal Chem* 1988;60:1193–1201.
41. Naes T, Martens H. Principle component regression in NIR analysis: viewpoints, background details, and selection of components. *J Chemom* 1988;2:155–67.
42. Dolmatova L, Ruckebusch C, Dupuy N, Huvenne JP, Legrand P. Quantitation analysis of paper coatings using artificial neural networks. *Chemom Intel Lab Syst* 1997;36:125–40.
43. Hong-kui X, Levine SP, D'Arcy JB. Iterative least-squares fit procedures for the identification of organic vapors mixtures by Fourier transform infrared spectrophotometry. *Anal Chem* 1989;61:2708–14.
44. Bauer WF, Connolly MJ, Rilling A, Gravel D, Perry S. Evaluation of Fourier transform infrared spectroscopy for the determination of volatile organic compounds in transuranic waste drum headspace. 1995 INEL Report No.: INEL-95/0332.

Additional information and reprint requests:

Garold L. Gresham
 Idaho National Engineering and Environmental Laboratory
 PO Box 1625
 Idaho Falls, ID 83415–2208